

A Comparison of Photocatalytic Activity of TiO₂ Nanocomposites Doped with Zn²⁺/Fe³⁺ and Y³⁺ Ions

Himanshu Narayan^{1,*} and Hailemichael Alemu²

¹Department of Physics & Electronics, National University of Lesotho, Roma 180, Lesotho.

²Department of Chemistry & Chemical Technology, National University of Lesotho, Roma 180, Lesotho.

(*) Corresponding author: h.narayan@nul.ls

(Received: 17 June 2016 and Accepted: 23 April 2017)

Abstract

TiO₂ based nanocomposites (NCs) were synthesized using the co-precipitation/hydrolysis (CPH) method. The composition of the first set (TZF) and the second set (TY) of NCs were: TiO₂.[ZnFe₂O₄]_x (with $x = 0.1$ to 0.5), and TiO₂.[Y₂O₃]_x (with $x = 0.1$ to 0.5), respectively. NCs with average crystallite size of 29 nm were produced when co-doped Zn²⁺/Fe³⁺ ions into TiO₂. This size was 17 nm when Y³⁺ ions were doped. Characterization of all samples were done by scanning electron microscopy (SEM), transmission electron microscopy (TEM), x-ray diffraction (XRD) and particle size analyzer. Visible light photocatalytic degradation of the dye Congo red (CR) was investigated in the presence of each of the samples. In comparison with pure TiO₂, enhanced photocatalytic activity was recorded with NCs. The NCs with $x = 0.2$ and $x = 0.1$ of TY and TZF sets, respectively, showed maximum photocatalysis both in terms of the apparent rate constant, as well as the percent degradation observed after 180 minutes. It was noted that enhanced photodegradation is directly related to the reduced particle size of the composites which implies that, photosensitization is the dominant process. The better photocatalytic activity observed with TY in comparison to with TZF NCs was attributed to the effective suppression of the e^-/h^+ recombination because of the trapping of photo-generated electron by the Y³⁺ ions.

Keywords: Titanium dioxide, Nanocomposite, Photocatalysis.

1. INTRODUCTION

Environmental pollution is a cost that every nation has to pay for industrial development. All industries, regardless to their size and scale of production, cause polluting the environment. For obvious reasons, air and water are the two natural resources that more polluted by industries. For example, textile and chemical industries are one of the most important producers of wastewater that containing several hazardous pollutants, such as organic dyes, phenols, poly-chloro-biphenyls (PCB's), and many other contaminates. One possible approach for the treatment of wastewater is the photocatalytic oxidative degradation of the pollutants, which is currently being studied by a number of groups around the globe.

The titanium oxide (TiO₂) with wide band gap ($E_g = 3.2$ eV) is a semiconductor material that has ability to degrade a wide variety of organic pollutants and also its photocatalytic properties were widely investigated. Even in the pure and commercially available form, TiO₂ shows considerable photocatalytic activity and further enhancement of its efficiency is possible by appropriate structural and compositional modifications. However, it is crucial to understand the processes involved in and also the factors influencing the TiO₂ mediated photocatalytic oxidation. According to the literature, the two generally accepted mechanisms [1, 2] are as follows:

(i) Photo-excitation: Irradiation with

wavelengths can excite electrons from the valence band (VB) to the conduction band (CB) of TiO₂, leaving behind the holes. Both these excited electrons and the holes can react with oxygen, water and hydroxide ions to form highly active oxygen species. These active species can react with the pollutants leading to their degradation. In this mechanism, the band-gap (E_g) of the semiconductor plays a major role.

(ii) Photosensitization: Pollutants (e.g., dyes) can get adsorbed to the TiO₂ particles and start absorbing visible radiations. Thus, they can get photochemically excited to transfer an electron to the TiO₂. Such a transfer can result into the formation of a superoxide anion radical from reduction of the molecular oxygen. At the same time, a cation radical can be produced from the pollutant, which may lead to the degradation of other pollutant molecules. This mechanism depends on the size (or, the effective surface area) of the TiO₂ particles.

The 3.2 eV band-gap of pure TiO₂ corresponds to a band-edge (or, cut-off wavelength, λ_{cutoff}) of about 390 nm, which falls inside the UV-region of the spectrum. So, the wavelengths larger than this value are not used in the excitation of VB electrons, and consequently visible light photocatalysis by photo-excitation is not possible. But, the pure material can be modified by some suitable methods such as doping to change band-gap structure for supporting visible light photocatalysis. In this direction, several authors have reported doping of TiO₂ with narrow band semiconductors, such as, CdS [3], CdSe [4], Fe₂O₃ [5], FeS₂ [6], RuS₂ [7], ZnFe₂O₄ [8, 9], Zn & S [10] etc. Furthermore, the specific surface area of TiO₂ can be increased by employing an appropriate method of synthesis, which can produce particles with reduced size in order to facilitate additional photosensitization. Studies along this line, e.g., with the nano-structures of pure TiO₂ [1, 11-14, 15], as

well as with nano-materials based on TiO₂ [9, 16, 17, 18], are also well documented.

Beside these, a third important factor, namely, the recombination of photo-generated electrons with the holes (e^-/h^+ recombination), also hampers the photocatalytic activity of the material significantly, and therefore, needs to be taken into account. Many research groups, have suggested various methods to control or minimize the effects of recombination. For example, doping of some transition metal ions (e.g., Fe³⁺, Cu²⁺, Mn²⁺, etc.) can enhance the photocatalytic activity, either by trapping photo-generated electrons in TiO₂ [19], or due to the formation of reactive complexes [20, 21].

Thus, as mentioned above, there are at least three important factors that significantly affect photocatalytic efficiency of TiO₂. Interestingly, they are interconnected with each other, especially when the particle size is reduced. For example, the smaller particle size may improve the photocatalytic activity of photocatalysts but may also reduce one or both other requirements. This is because of quantum size effect [22] that makes band-gap wider than bulk for very small particles (size < 10nm). As a result, the λ_{cutoff} could actually decrease, instead of increasing towards the visible regions. Similarly, the e^-/h^+ recombination could also become significantly high at smaller dimensions [10] because of the smaller 'free-path' available, and that could result in further reduction of the photocatalytic activity. Therefore in order to achieve optimum efficiency, one needs to strike a balance between these three decisive factors.

Recently, we have reported that modification of band-gap may be considered as the least important factor among the three, in some TiO₂ based NCs [23]. We have argued that in TiO₂.[ZnFe₂O₄]_x NCs, the band-gap modification may not be contributing much to the observed improvement of photocatalytic activity as reported by some

authors [8]. Rather, it could be apparently because the presence of metal ions (Zn^{2+} and Fe^{3+}) significantly inhibits the e^-/h^+ recombination. Thus, we have concluded that even if the band-gap is not narrowed by doping, the visible light photocatalysis can still progress through photosensitization, and can still be improved by reducing the particle size (or effectively, by increasing the specific surface area).

With the above mentioned background, we revisit some of our already reported results, combine them with some unpublished ones, and present a comparative analysis of the observations. Primarily with respect to the role of two factors, i.e., particle size and e^-/h^+ recombination, in the improvement of photocatalytic activity of TiO_2 , we present the results obtained with $TiO_2.[Y_2O_3]_x$ (or, TY) NCs mediated photocatalytic degradation of the dye Congo red (CR) as against that obtained with $TiO_2.[ZnFe_2O_4]_x$ (or, TZF) NCs.

It is noteworthy to mention here that Y_2O_3 (or, Y^{3+} ions) was deliberately chosen as the dopant in our investigations, because of its band-gap of about 4.5 eV ($\lambda_{cutoff} = 275$ nm) [24], which is wider than that of pure TiO_2 . In the composites thus synthesized, the possibility of visible light photocatalysis by photo-excitation can be thoroughly ruled out since they are not expected to absorb in the visible regions of the spectrum. Consequently, the effects of photosensitization can be investigated exclusively. Additionally, Y^{3+} ions doping is also expected to enhance photocatalytic activity by suppressing the undesired e^-/h^+ recombination as the rare earth ions, such as Ce^{4+} and Eu^{3+} , are known for efficiently trapping the electrons [25-27]. However, as evident from the inadequate published work available, this area of research, especially the studies related to the photocatalytic properties of Y^{3+} ions doped TiO_2 is still very much open, possibly with a lot of promising results.

2. EXPERIMENTAL

2.1. Materials Synthesis

The method of co-precipitation/hydrolysis (CPH) can be employed to synthesize doped TiO_2 NCs [8, 23, 28]. Usually the starting material is nitrate of the corresponding dopant because of its high solubility. Detailed methods for the preparation of rare-earth ions doped TiO_2 NCs have been reported by us elsewhere [28-30].

Chemicals used for the synthesis of TZF series of NCs ($x = 0.1, 0.2, 0.3, 0.4$ and 0.5) were $Fe(NO_3)_3 \cdot 9H_2O$ and $Zn(NO_3)_2 \cdot 4H_2O$ (from HOLPRO ANALYTICS, SA), n-propanol (BDH), iso-propanol (UNILAB, SA), tetrabutyl-orthotitanate (Fluka), and nitric acid (ACE, SA). For the TY series of NCs ($x = 0.1, 0.2, 0.3, 0.4$ and 0.5) $Y(NO_3)_3 \cdot 6H_2O$ (from Riedel-de Haën) was used as the starting nitrate. To precipitate the nitrate precursor, the pH of the solution was raised to 6.5 by slowly adding a 3.5 M NH_4OH solution using isopropyl alcohol as the solvent. Approximately 10 g of distilled and deionized water was then added drop wise to the solution and was stirred for 45 minutes. A solution of tetrabutyl-orthotitanate [$Ti(OBu)_4$] and isopropyl alcohol was prepared in a ratio of 1:2 by weight and added drop wise to the co-precipitated Y_2O_3 solution for controlled hydrolysis with H_2O : $Ti(OBu)_4$ in the ratio of 25:1. The final solution was kept stirred at 65 °C for 90 minutes, filtered, and then dried at 100 and 220 °C, respectively. The prepared TY nanoparticles were then calcined in a flowing air atmosphere at 500 °C for three hours. Following the same steps and starting with their respective nitrates [29, 30], other rare-earth ions (Yb, Gd, Er, Nd, etc.) doped NCs can also be prepared. The Congo red dye used in the photocatalytic degradation experiments was obtained from Aldrich Chemical Co.

2.2 Measurements

All the samples were characterized by Transmission electron microscopy (TEM),

scanning electron microscopy (SEM), particle-size analysis and powder x-ray diffraction (XRD). The TEM was carried out on a Philips CM200 TEM instrument (FEI Co.) and SEM, on a Jeol JSM5600 machine. Powder x-ray diffraction (XRD) was done on a Shimadzu D6000 diffractometer (Shimadzu, Japan) using Cu-K α radiation ($\lambda = 1.5406 \text{ \AA}$). The particle size distribution of the composites was measured as water suspension using a Microtrac/Nanotrac TM150 particle size analyzer, which employs optical light scattering measurements.

The visible-light photoactivity was carried out in an inexpensive, locally fabricated photoreactor [23]. An experimental solution (850 ml) containing 25 mg of Congo red per liter of water, a stirring bar, and 275 mg of photocatalyst sample was placed in the photoreactor. The fluorescent lamp was turned on and the

solution was stirred throughout the duration of the experiment. At predetermined times, 1.5 ml of the solution was removed and centrifuged. The clear solution was taken and its absorbance was measured at 498 nm using a UV-Vis Shimadzu model 1201 spectrophotometer. The absorbance of the Congo red solutions in the presence of photocatalyst sample without light, and, with light but in the absence of the sample were also measured to see the dependence of degradation of the dye in the presence of catalyst and light alone, respectively. The photocatalytic properties of the NCs were thus measured for the decomposition of Congo red under visible light irradiation.

3. RESULT AND DISCUSSION

3.1 Estimation of Particle Size

Both the TEM and SEM pictures (depicted in Fig. 1) clearly show that larger grains of the NCs are agglomeration

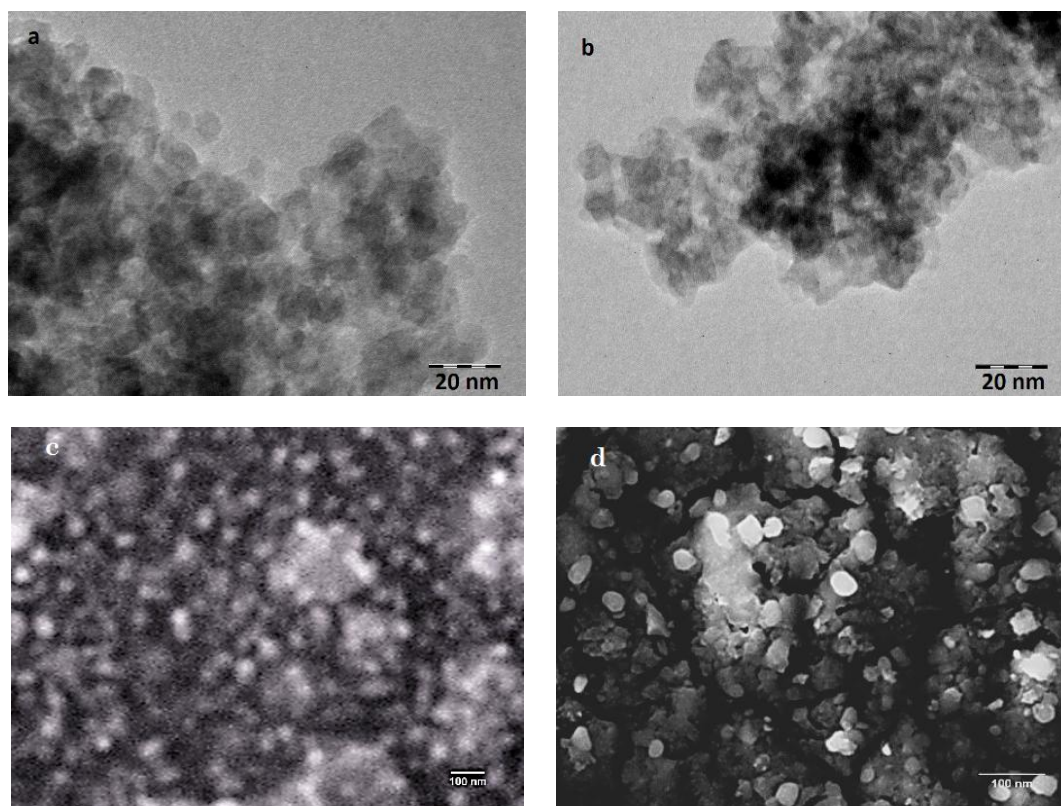


Figure 1. Transmission electron microscopy pictures of (a) $\text{TiO}_2\text{.[ZnFe}_2\text{O}_4]_{0.1}$ and (b) $\text{TiO}_2\text{.[Y}_2\text{O}_3]_{0.1}$ NC samples, and scanning electron microscopy pictures of (c) $\text{TiO}_2\text{.[ZnFe}_2\text{O}_4]_{0.1}$ and (d) $\text{TiO}_2\text{.[Y}_2\text{O}_3]_{0.1}$ NC samples.

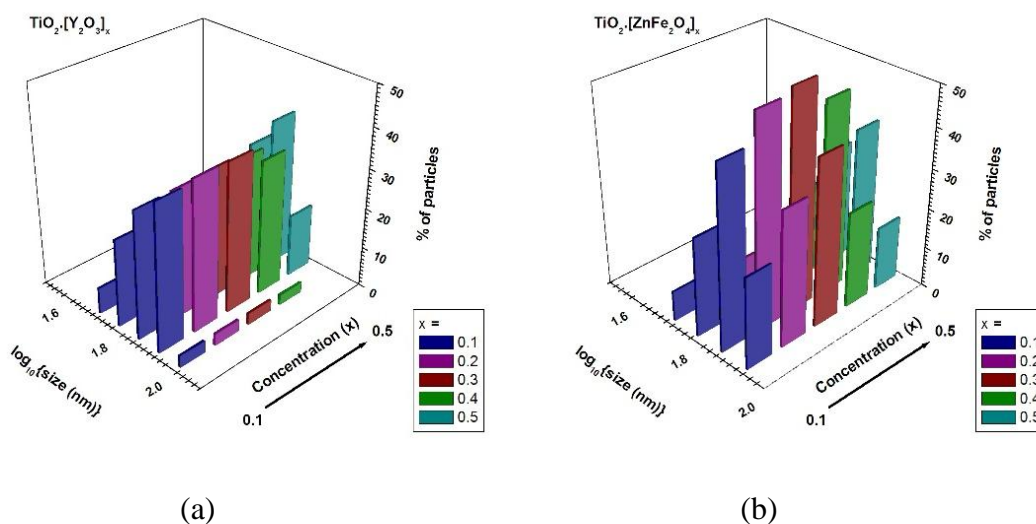


Figure 2. Distribution of particle size for all the NC samples of (a) $\text{TiO}_2\cdot[\text{Y}_2\text{O}_3]_x$, and (b) $\text{TiO}_2\cdot[\text{ZnFe}_2\text{O}_4]_x$.

of smaller particles. These pictures also give a rough estimate of the grain size of the composites around 70 nm. A more precise measurement of the grain size was carried out using the particle size analyzer. Figure 2 shows the distribution of number of particles with size. The average particle size of the TY composites was almost uniform for all the samples around 74 nm. In the NC samples of the TZF set, an almost uniform range of particle size was determined averaging at about 72 nm. The average size of the NCs for both TY and TZF sets was thus comparable to that size estimated from the SEM pictures. The average grain size of the commercial rutile and anatase TiO_2 was also estimated and found to be about 4.03 and 2.44 μm , respectively. The grain size for all the samples measured on the size-analyzer is summarized in Table 1.

Figure 3 shows the XRD results for the TY and TZF sets of NCs with $x = 0.1$ and $x = 0.2$ compositions. The spectra for crystalline TiO_2 (both anatase and rutile phases), and Y_2O_3 are also shown in order to facilitate proper identification of the peaks. The obvious and sharp peaks indicate the crystalline nature of the samples and hence facilitate the identification of various phases of

precursor powders in the composites. Thus, with the increasing value of x in these samples, a gradually decreasing amount of TiO_2 is revealed by the decreasing height of the $2\theta = 25.7^\circ$ (101) anatase peak. Other anatase peaks, although most of them highly broadened, and/or merged with the peaks of other phases also point towards the presence of this phase in all the NCs. On the other hand, the gradual increase of Y_2O_3 with x in the samples is indicated by the increasing heights of the $2\theta = 29.22^\circ$ (222), 33.8° (400), 48.6° (440) and 57.7° (622) peaks of the oxide. In the TZF composites with the increasing value of x , a similar decrease of rutile phase is revealed by the decreasing heights of the characteristic peaks. Moreover, with increasing x , the increasing ratios of ZnO and Fe_2O_3 are indicated by the gradually increasing heights of the corresponding peaks at $2\theta = 31.8^\circ$ (100), and 34.5° (002) peaks of ZnO, and 33.6° (104) peak of Fe_2O_3 .

In the XRD data for both TY and TZF sets of NCs, an obvious broadening of the prominent peaks indicates directly to the reduced size of the particles. This is also confirmed from the results of crystallite size calculated from XRD data, as discussed in the next paragraph.

Nonappearance of any new peak in the plots for the NCs shows that no new phase was formed during the process of synthesis. Further, the absence of any meaningful shift in the peak positions with respect to those corresponding to the starting materials reveals that the dopant ions have not replaced or substituted the ions in host TiO_2 lattice, and therefore the host lattice structure has not changed due to doping.

From the broadening of the observed peaks, the mean crystallite (defined as the smallest regions of the sample that diffract the incident x-rays coherently) size z of the samples were estimated using the Debye-Scherrer formula [16, 11, 31]. The FWHM of the Gaussian best-fit to the prominent peaks in the XRD data was used as the broadening parameter. It was found that z for the as received rutile and anatase TiO_2 was 52 and 57 nm, respectively. For the TY composites, the average crystallite size was determined to be 17 nm for all NC samples. On the other hand, average crystallite size was estimated to be around 29 nm for the TZF NC samples [see Table 1]. To avoid confusion, it is noteworthy to mention here that because of the difference

of probes used in the measurements, the ‘crystallite-’ and ‘particle-’ size have different meanings. In the particle size analyzer, optical light scattered from the small grains, suspended in solution, is used in the determination of particle (or, grain) size. This is the size visible under the microscopes, e.g. SEM, that use reflection of the probes to construct the image. However, since the x-rays can penetrate through the surface of the particles, what is measured through XRD is actually the size of the small domains (the so called ‘crystallites’) within the grains that diffract the x-rays coherently [32]. TEM images shown in Fig. 1 also indicate that the crystallites (smaller particles) of roughly 20 nm size agglomerate into bigger grains. In a powdered sample, one particle can obviously have several crystallites within itself. A comparison of the crystallite size (determined by XRD) and the particle size (measured by particle size analyzer), in the three-dimensional geometry, seems to reveal that about 80 crystallites agglomerate to make one particle of the TY NCs, whereas only about 15 combine together to make a TZF NC particle.

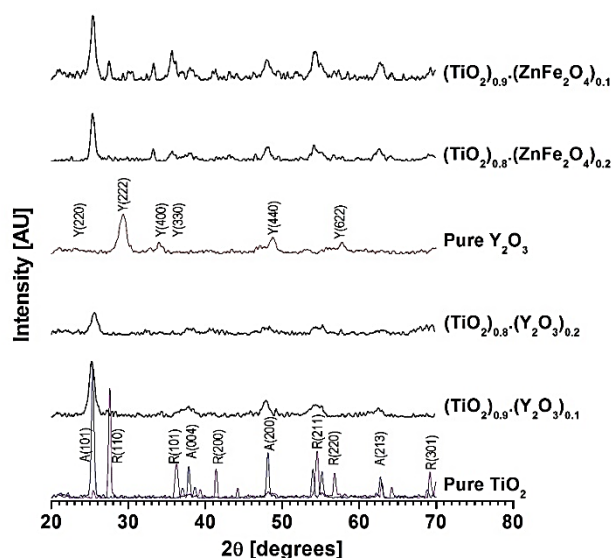


Figure 3. X-ray diffraction data shown for $x = 0.1$ and $x = 0.2$ compositions of the NCs, along with the peak positions corresponding to pure TiO_2 (A: Anatase and R: Rutile phases) and Y_2O_3 powders.

3.2 Photocatalytic Activity

The photocatalytic activity of both TY and TZF sets of composites under the visible light ($\lambda > 420$ nm) was examined for the degradation of the dye Congo red (CR). Figure 5 shows the degradation in terms of the relative concentration of CR as a function of time for the composites with better photocatalytic properties along with that for the commercial TiO_2 . No obvious degradation of CR was observed with the composites in the absence of irradiation, as well as under irradiation but without any photocatalyst.

For all the three types of photo-catalytic materials, namely the TY and TZF sets and the commercial TiO_2 the rate of degradation of CR was found to be of first order. The apparent rate constant (k_{obs}) for the degradation process was estimated from a least-square regression of $\ln(C/C_0)$ vs time.

All the TY NC samples showed substantial degradation of CR. After 180 minutes, the $x = 0.1, 0.2, 0.3$ and 0.4 samples degraded 91%, 95%, 92% and 86% of CR, respectively. In terms of the apparent rate constant however, the fastest

initial degradation was observed for the TY NCs with $x = 0.1$ with a value of $k_{\text{obs}} = 2.74 \times 10^{-2} \text{ min}^{-1}$, which was only marginally higher than that for $x = 0.2$ composition with $k_{\text{obs}} = 2.62 \times 10^{-2} \text{ min}^{-1}$. At these rates, both these TY NCs degraded the CR to half of its initial concentration in less than 30 minutes. On the other hand, the TZF NCs showed less photocatalytic activity as compared to the TY NCs. The best performance, both in terms of the rate, as well as the percent degradation after 180 minutes, was observed for the $x = 0.1$ composition of TZF NCs. For this sample, the rate $k_{\text{obs}} = 1.60 \times 10^{-2} \text{ min}^{-1}$ was estimated with about 90% of CR degradation after 180 minutes. The $x = 0.2$ composition of this set also showed considerable photocatalytic activity, degrading 86% of CR in 180 minutes, and with the rate $k_{\text{obs}} = 1.57 \times 10^{-2} \text{ min}^{-1}$, which was slightly better than about 85% degradation observed with commercial pure anatase TiO_2 . The TZF NCs took a little more than 30 minutes to degrade the CR to half of its initial concentration.

All other samples of TY and TZF sets

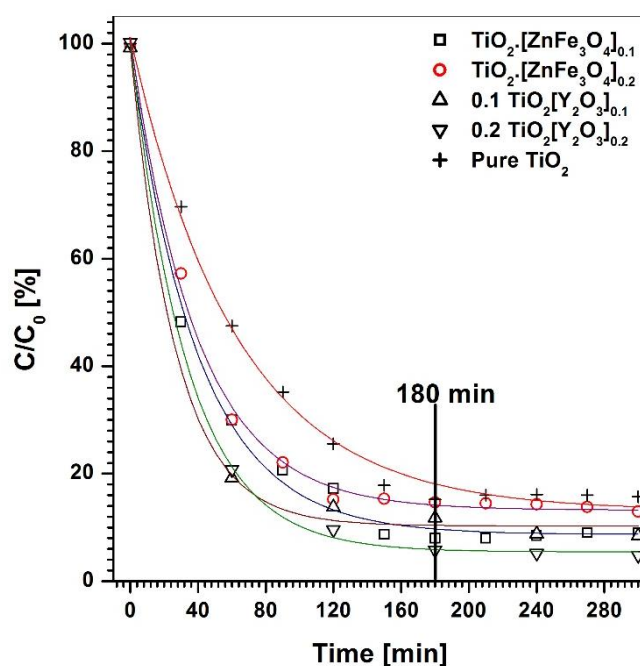


Figure 4. Photocatalytic degradation of Congo red dye in the presence of various nano-composites.

performed worse than the commercial TiO₂, and therefore, not discussed here in detail. The best photocatalytic activity is shown by the compositions with $x \leq 0.2$ points towards the possible existence of an optimum dopant concentration around $x = 0.2$ for the best performing photocatalyst. Beyond this optimum concentration, the photocatalytic activity decreases, probably due to the effective reduction of relative concentration of active part in the composite, i.e., of the host TiO₂ itself. More work about a better understanding of this optimum doping is in progress.

Some interesting conclusions may be drawn from these results of photocatalytic degradation of CR. First, the role of band gap modification in the photocatalytic degradation, at least in the present example, is apparently negligible. This conclusion is based on the fact that only in the TZF set, the band-gap was favorably modified. For example, in comparison to the 390 nm limit (λ_{cutoff}) for pure TiO₂, the useful part of the spectrum was extended up to $\lambda_{\text{cutoff}} = 420$ nm and 445 nm (more towards the visible region) respectively for $x = 0.1$ and 0.2 molar concentration of ZnFe₂O₄ doping [8]. However, this modification has apparently no significant effect on the observed photocatalytic activity of the materials, because beyond $x = 0.2$, it was found to decrease rapidly, although with more doping the value of λ_{cutoff} was expected to increase further into the visible regions of the spectrum.

Secondly, the crystallite-size z clearly plays a very important role in the photocatalysis. Nano-sized samples of both TY (average grain-size $b = 74$ nm, crystallite-size $z = 17$ nm) and TZF ($b = 72$ nm, $z = 29$ nm) sets have shown better degradation than the pure TiO₂. Therefore, photosensitization seems to be the process that is primarily responsible for the visible light photocatalytic degradation of CR in the presence of TiO₂ based materials. Smaller particle size is directly related to larger specific surface area available to the dye molecules to get adsorbed on the catalyst particles. After getting adsorbed on the surface, the dye molecules start absorbing the visible light (wavelengths < 500 nm for CR) and get photochemically excited, which eventually leads to their degradation.

The third key implication emerges as a consequence of following considerations: The highest photocatalytic activity in the degradation of CR has been observed with the TZF NCs with molar concentration $x = 0.1$ of ZnFe₂O₄ (notably, $x = 0.2$ of this set also showed significant photodegradation) and beyond this, it decreased. This shows that ZnFe₂O₄ as a material plays only a little role in the improvement of photocatalytic properties of the composites, possibly because of its short photoactive lifetime [8]. Therefore in this set, the observed better degradation of CR can be attributed mainly to the smaller particle size. However, in the TY set all the

Table 1. Summary of results.

Sample	x	Crystallite size (z)	Particle size (b)	k_{obs} ($\times 10^{-2} \text{ min}^{-1}$)	Degradation in 180 minutes	Comments
Anatase TiO ₂		57 nm	2.44 μm	1.07	85%	As received
Rutile TiO ₂		52 nm	4.03 μm	1.07	80%	
TiO ₂ ·[Y ₂ O ₃] _x	0.1	16 nm	74 nm	2.74	91%	Synthesized by co-precipitation/hydrolysis
	0.2	19 nm	75 nm	2.62	95%	
	0.3	16 nm	75 nm	1.71	92%	
	0.4	16 nm	73 nm	1.52	86%	
TiO ₂ ·[ZnFe ₂ O ₄] _x	0.1	29 nm	71 nm	1.60	90%	
	0.2	29 nm	75 nm	1.57	86%	
	0.3	30 nm	77 nm	0.75	73%	
	0.4	29 nm	72 nm	0.11	35%	

The crystallite size z was measured from XRD data, and the particle size b was measured from particle size analyzer.

NCs showed significant photocatalytic activity (more than 90% degradation of CR after 180 minutes for molar concentration $x \leq 0.3$), with the highest degradation recorded with $x = 0.2$ sample. As mentioned earlier, the band gap modification cannot be held responsible for the improved visible light induced photocatalytic activity of this set. The wide band-gap of about 4.5 eV ($\lambda_{\text{cutoff}} = 275$ nm) [24] of pure Y_2O_3 corresponds to the requirement of UV (UV-C range or 280 – 100 nm) irradiation to initiate photocatalysis [33], and therefore it is practically inactive under the present experimental conditions with visible light. In other words, Y_2O_3 is not directly involved in the visible light photocatalytic degradation of CR. Therefore, it follows that the smaller particle size is the factor primarily responsible for the better photocatalytic activity of TY NCs. However, a more careful analysis in terms of the average particle sizes of the best performing NCs from both sets seems to suggest that there could be another factor that is positively influencing the visible light photocatalysis with the TY samples. The TZF composite ($x = 0.1$) with 71 nm size showed 90% (with the rate $k_{\text{obs}} = 1.60 \times 10^{-2} \text{ min}^{-1}$), whereas TY composite ($x = 0.2$) with marginally bigger size of 75 nm produced 95% ($k_{\text{obs}} = 2.62 \times 10^{-2} \text{ min}^{-1}$) degradation after 180 minutes. It should have been an opposite trend, both in terms of percent degradation and the apparent rate constant, if particle size was the sole reason for better performance of the TY NCs. Therefore, besides the smaller particle size, the enhanced photocatalytic activity of TY NCs under visible light may be attributed to some other factors also. One such possible factor may be the suppressed e^-/h^+ recombination in the presence of Y^{3+} ions, since the rare earth ions can efficiently trap the photogenerated electrons. These observations were later supported by some of our investigations with rare-earth ions (such as, Er^{3+} and Nd^{3+}) doped TiO_2 NCs that produced close

to 100% degradation of Congo red at a very fast rate under similar experimental conditions [32].

Finally, in support of the apparent role of Y^{3+} ions in the inhibition of e^-/h^+ recombination, it is noteworthy to mention that for higher molar concentration of the dopants ($x \geq 0.2$), the decrease in photocatalytic activity of both sets of the samples does not seem to be directly associated with the anatase to rutile conversion as claimed by some authors [8]. Liu et al [34] have suggested that coexistence of anatase and rutile has higher efficiency for the degradation of Rhodamine B than that with the anatase phase alone. Therefore, if the presence of both phases of TiO_2 has any effect on the photocatalytic activity, expectedly it should be positive. We believe that the higher dopant concentration ($x \geq 0.2$) effectively reduces the active part of the catalyst leading to decreased photocatalytic activity. This observation is adequately supported by the XRD results, which also shows no such conversion from anatase to rutile taking place at higher dopant concentration.

3. CONCLUSION

The photocatalytic properties of TiO_2 can be significantly improved by suitable doping and by employing a method of synthesis that produces particles with reduced size. We have reported in this paper about the photocatalytic degradation of Congo red using TiO_2 doped with Y^{3+} ions (TY set), in comparison with that doped with $\text{Zn}^{2+}/\text{Fe}^{3+}$ ions (TZF set). In both the TY and TZF sets, NCs with molar doping $x = 0.1$ and 0.2 showed much enhanced photocatalytic degradation, but overall, the Y^{3+} ions doping resulted in superior photocatalysts. This observation directly proved the importance of smaller particle size for better photocatalytic properties. Further, the analysis of results pointed to the existence of an optimum doping concentration around molar doping $x = 0.2$. Above this, the doping seems to

worsen the photocatalytic activity instead of enhancing. A more careful analysis of the results indicated that in the TY nanocomposites, the doping of Y^{3+} ions supports the process of photocatalytic degradation, apparently by inhibiting the undesired e^-/h^+ recombination.

ACKNOWLEDGEMENTS

The authors would like to thank Mr. Lebohang Macheli for sample preparation and some measurements, and to Professor Madhavi Thakurdesai, Department of Physics, Birla College, Kalyan, India for her help in microscopy of some of the samples.

REFERENCES

1. Bumpas J.A., Tricker J., Andrzejewski K., Rhoads H., Tatarko M. (1999). "Remediation of water contaminated with an azo dye: An undergraduate laboratory experiment utilizing an inexpensive photocatalytic reactor", *Journal of Chemical Education*, 76(12): 1680-1683.
2. Uyguner Ceyda Senem, Bekbolet Miray (2007). "Contribution of metal species to the heterogeneous photocatalytic degradation of natural organic matter", *International Journal of Photoenergy*, Article ID 23156.
3. Vogel Ralf, Pohl Klaus, Weller Horst (1990). "Sensitization of highly porous, polycrystalline TiO_2 electrodes by quantum sized CdS", *Chemical Physics Letters*, 174(3-4): 241-246.
4. Liu D., Kamat P.V. (1993). "Photoelectro-chemical behaviour of thin cadmium selenide and coupled titania/cadmium selenide semiconductor films", *The Journal of Physical Chemistry*, 97(41): 10769-10773.
5. Banisharif A., Hakim Elahi S., Anaraki Firooz A., Khodadadi A.A., Mortazavi Y. (2013). " TiO_2/Fe_3O_4 Nano-composite Photocatalysts for Enhanced Photo-Decolorization of Congo Red Dye", *International Journal of Nanoscience and Nanotechnology*, 9(4): 193-202.
6. Ennaoui A., Fiechter S., Tributsch H., Giersig M., Vogel R., Well H. (1992). "Photoelectro-chemical energy conversion obtained with ultrathin organo – metallic – chemical – vapour – deposition layer of FeS_2 (Pyrite) on TiO_2 ", *Journal of Electrochemical Society*, 139: 2514-2518.
7. Ashokkumar M., Kudo A., Saito N., Sakata T. (1994). "Semiconductor sensitization by RuS_2 colloids on TiO_2 electrodes", *Chemical Physics Letters*, 229(4-5): 383-388.
8. Srinivasan Sesha S., Wade Jeremy, Stefanakos Elias K. (2006). "Synthesis and Characterization of Photocatalytic $TiO_2-ZnFe_2O_4$ Nanoparticles", *Journal of Nanomaterials*, Article ID 45712.
9. Yuan Z.-H., Zhang L.-d. (2001). "Synthesis, characterization and photocatalytic activity of $ZnFe_2O_4/TiO_2$ nanocomposite", *Journal of Materials Chemistry*, 11: 1265-1268.
10. Qianzhi Xu, Xiuying Wang, Xiaoli Dong, Chun Ma, Xiufang Zhang, Hongchao Ma. (2015). "Improved visible light photocatalytic activity for TiO_2 nanomaterials by codoping with zinc and sulfur", *Journal of Nanomaterials*, Article ID 157383.
11. Wahi R.K., Yu W.W., Liu Y., Mejia M.L., Falkner J.C., Nolte W., Colvin V.L. (2005). "Photodegradation of Congo red catalyzed by nanosized TiO_2 ", *Journal of Molecular Catalysis A: Chemical*, 242: 48-56.
12. Khan M.A., Jung H.-T., Yang O.-B. (2006). "Synthesis and Characterization of Ultrahigh Crystalline TiO_2 Nanotubes", *Journal of Physical Chemistry B*, 110: 6626-6630.
13. Dung N.T., Khoa N.V., Herrmann J.M. (2005). "Photocatalytic degradation of reactive dye RED-3BA in aqueous TiO_2 suspension under UV-visible light", *International Journal of Photoenergy*, 07: 11-15.
14. Qingchi Xu, Jiabin Zeng, Xingyun Li, Jun Xu, Xiangyang Liu. (2016). "3D nano-macroporous structured TiO_2 -foam glass as an efficient photocatalyst for organic pollutant treatment", *RSC Advances*, 6: 51888-51893.
15. Mehrizad A., Gharbani P. (2011). "Study on Catalytic and Photocatalytic Decontamination of (2-Chloroethyl) Phenyl Sulfide with Nano- TiO_2 ", *International Journal of Nanoscience and Nanotechnology*, 7(1): 48-53.
16. Habibi M.H., Esfahani M.N., Egerton T.A. (2007). "Photochemical Characterization and Photocatalytic Properties of a Nanostructure Composite TiO_2 Film", *International Journal of Photoenergy*, Article ID 13653.
17. Cheng P., Li W., Zhou T., Jin Y., Gu M. (2004). "Physical and photo-catalytic properties of zinc ferrite doped titania under visible light irradiation", *Journal of Photochemistry and Photobiology A: Chemistry*, 168: 97-101.
18. Soroodan Miandoab E., Fatemi Sh. (2015). "Upgrading TiO_2 Photoactivity under Visible Light by Synthesis of MWCNT/ TiO_2 Nanocomposite", *International Journal of Nanoscience and Nanotechnology*, 11(1): 1-12.
19. Ward Michael D., Bard Allen J. (1982). "Photocurrent enhancement via trapping of photogenerated electrons of TiO_2 particles", *Journal of Physical Chemistry*, 86: 3599-3605.

20. Butler Elizabeth C., Davis Allen P. (1993). "Photocatalytic oxidation in aqueous titanium dioxide suspensions: the influence of dissolved transition metals", *Journal of Photochemistry and Photobiology A: Chemistry*, 70(3): 273-283.
21. Wei Tsong-Yang, Wang Yung-Yun, Wan Chi-Chao (1990). "Photo-catalytic oxidation of phenol in the presence of hydrogen peroxide and titanium dioxide powders", *Journal of Photochemistry and Photobiology A: Chemistry*, 55(1): 115-126.
22. Satoh Norifusa, Nakashima Toshio, Kamikura Kenta, Yamamoto Kimihisa (2008). "Quantum size effect in TiO₂ nanoparticles prepared by finely controlled metal assembly on dendrimer templates", *Nature Nanotechnology*, 3(2): 106-111.
23. Narayan Himanshu, Alemu Haile-michael, Macheli Lebohang, Sekota Mantoa, Thakurdesai Madhavi, Gundu Rao T.K. (2009). "Role of particle size in visible light photocatalysis of Congo red using TiO₂[ZnFe₂O₄]_x nanocomposites", *Bulletin of Materials Science*, 32(5): 499-506.
24. Xu Yong-Nian, Gu Zhong-quan, Ching W.Y. (1997). "Electronic, structural, and optical properties of crystalline yttria", *Physical Review B*, 56(23): 14993-15000.
25. Liu Jianhua, Yang Rong, Li Songmei (2007). "Synthesis and Photocatalytic Activity of TiO₂/V₂O₅ Composite Catalyst Doped with Rare Earth Ions", *Journal of Rare Earths*, 25(2): 173-178.
26. Xie Yibing, Yuan Chunwei (2004). "Characterization and photocatalysis of Eu³⁺-TiO₂ sol in the hydrosol reaction system", *Materials Research Bulletin*, 39(4-5): 533-543.
27. Guan K.-s., Yin Y.-s. (2005). "Effect of rare earth addition on super-hydrophilic property of TiO₂/SiO₂ composite film", *Materials Chemistry and Physics*, 92(1): 10-15.
28. Narayan Himanshu, Alemu Haile-michael, Macheli Lebohang, Thakurdesai Madhavi, Gundu Rao T.K. (2009). "Synthesis and characterization of Y³⁺-doped TiO₂ nanocomposites for photocatalytic applications", *Nanotechnology*, 20: 255601 (8pp).
29. Narayan Himanshu, Alemu Haile-michael, Alotsi Daniel N., Macheli Lebohang, Thakurdesai Madhavi, Jaybhaye Sandesh, Singh Arvind (2012). "Fast and complete degradation of Congo red under visible light with Er³⁺ and Nd³⁺ ions doped TiO₂ nanocomposites", *Nanotechnology Development*, 2:e, 5-11.
30. Narayan Himanshu, Alemu Haile-michael, Setofolo Lijeloang, Macheli Lebohang (2012). "Visible Light Photocatalysis with Rare Earth Ion-Doped TiO₂ Nanocomposites", *ISRN Physical Chemistry*, 2012: Article ID 841521, 9 pages.
31. Boulc'h F., Schouler M.-C., Donnadiou P., Chaix J.-M., Djurado E. (2001). "Domain size distribution of Y-TZP nano-particles using XRD and HRTEM", *Image Analysis and Stereology*, 20: 157-161.
32. Dinnebier Robert E., Billinge Simon J.L., (2008). "Powder Diffraction: Theory and Practice", Royal Society of Chemistry. Chapter 5, 142.
33. Karunakaran C., Dhanalakshmi R., Anilkumar P. (2009). "Degradation of carboxylic acids on Y₂O₃ surface under UV light. Synergism by semi-conductors." *Radiation Physics and Chemistry*, 78(3): 173-176.
34. Liu G.-g., Zhang X.-z., Xu Y.-j., Niu X.-s., Zheng L.-q., Ding X.-j. (2004). "Effect of ZnFe₂O₄ doping on the photocatalytic activity of TiO₂", *Chemosphere*, 55: 1287-1291.